Extrapolation of Radiation Pattern with Neural Networks: A Paradigm with LSTM-based and Generative Adversarial Networks

(Article begins on next page)

Extrapolation of Radiation Pattern with Neural Networks: A Paradigm with LSTM-based and Generative Adversarial Networks

Lida Kouhalvandi[1△], Mohammad Alibakhshikenari[2+], Hassan Zakeri[3◇],
Ladislau Matekovits[4#], Serdar Ozoguz[5++], Takfarinas Saber[6‡], Ernesto Limiti[7+]
△ *Dept. of Electrical and Electronics Engineering, Dogus University, Istanbul, Turkiye*
+ *Electronics Engineering Department, University of Rome "Tor Vergata", 00133 Rome, Italy*
◇ *Dept. of Electrical Engineering, Amirkabir University of Technology, Tehran, Iran*
Dept. of Electronics and Telecommunications, Politecnico di Torino, Turin, Italy
++ *Dept. of Electronics and Communication Engineering, Istanbul Technical University, Istanbul, Turkiye*
‡ *Lero, Science Foundation Ireland Centre for Software, School of Computer Science, University of Galway, Galway, Ireland*
lida.kouhalvandi@ieee.org[1], alibakhshikenari@ing.uniroma2.it[2], h.zakeri@aut.ac.ir[3],
ladislau.matekovits@polito.it[4], ozoguz@itu.edu.tr[5], takfarinas.saber@universityofgalway.ie[6], limiti@ing.uniroma2.it[7]

Abstract—**The radiation pattern (RP) specification is an important graphical representation of diverse quantities such as directivity, gain, or electric field/power density in various antenna designs. Hence, optimizing the RP will effectively influence the overall performance of any communication system. calculating the RP in both the E-plane and H-plane is time-consuming and requires additional effort with simulations, since the calculations require the knowledge of the surface current on the overall structure. To tackle this drawback, we propose impressive methodologies for achieving the RPs through neural network-based approaches: generative adversarial network (GAN), and long short-term memory (LSTM)-based deep neural network (DNN). These two networks are strong enough to predicting the RP specifications at specific frequencies. To prove the effectiveness of the proposed method, a frequency-selective surface structure operating at the X-band is designed and afterward, the RPs are predicted through the two proposed networks (i.e., GAN and LSTM-based DNN) at 10.5 GHz which shows good agreement.**

Index Terms—**Antenna, deep neural network (DNN), forecasting, generative adversarial network (GAN), long short-term memory (LSTM), radiation pattern (RP).**

I. Introduction

Antennas are fundamental components used for various applications such as remote sensing, satellite communications, radio frequency identification, and wireless power transfer [1], [2]. For modern wireless communications, electromagnetic (EM) optimizations are taking the attention of antenna designers leading to achieving the optimal solutions in terms of specifications such as S-parameters, radiation patterns (RPs), gain, and so on. Hence, optimizing antennas is required to get highly directional performances [3]. Recently, various studies have been reported that focus on the optimization methods used for antenna designs.

In [4], a convex relaxation iterative optimization is employed as a solution for grating lobe suppression in antenna designs. The Pareto optimization method is applied in [5] for designing the elements of an antenna array along with their feed weights. For sideband radiation suppression, in [6] a methodology as the probability-based time-modulated array is presented to achieve suitable RPs. For reconfigurable multiple-input multiple-output (MIMO) antenna array, in [7] a sequential optimization framework with manifold optimization and eigenvalue decomposition is presented for obtaining maximization pattern design. In another study, [8], the excitation optimization technique is employed for enhancing the array isolation. The dynamic convex optimization is employed in [9] leading to array synthesis and providing a good initial starting point. For sparse conformal arrays, an improved snake optimization is presented in [10] for the beamforming design with the targets of decreasing the array element number and obtaining the best sparse array structure. There are various reported EM-based optimization methods in recent years which are mostly time-consuming and require massive analyses [11]. To tackle these drawbacks, machine learning (ML) methods for accelerating the optimization process and facilitating complicated design steps prove their effectiveness recently [12], [13].

This work is devoted to presenting two effective neural networks (NNs) based methodologies leading to the prediction of the RPs in both E and H-planes. Here, the generative adversarial network (GAN) and also long short-term memory (LSTM)-based deep neural network (DNN) are presented for being trained and for estimating the RPs at the specific frequency(ies). The effectiveness of the presented method is validated by first designing a frequency selective surface (FSS) structure and then training two determined NNs for estimating E-plane and H-plane RPs at 10.5 GHz frequency. The accuracies of trained networks are validated by making comparisons with the simulation results. This paper is organized as follows: Section II presents the methodology for predicting the RPs at the specific frequency(ies). The presented methods are verified in Sec. III by designing and optimizing an FSS structure and predicting the RPs for this configuration. Finally, Sec. IV

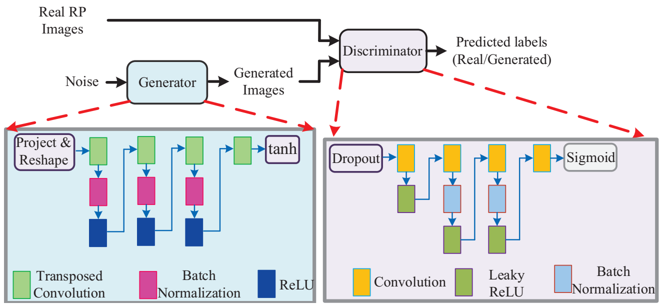

Fig. 1. General configuration of GAN.

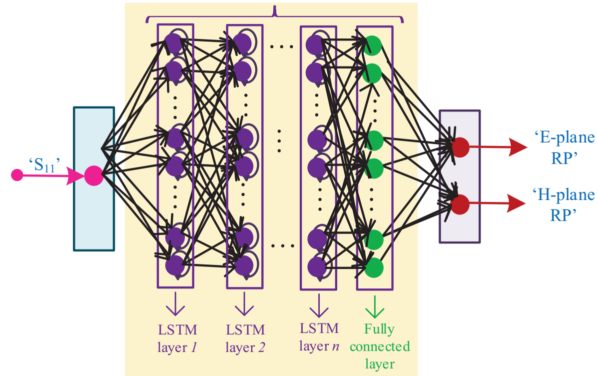

Fig. 2. LSTM-based DNN for predicting the RPs.

concludes this work.

II. Two NN-based Methods for Predicting RPs

As previously mentioned, extraction of RPs in both E-plane and H-planes especially for high-dimensional designs is time-consuming and needs additional effort. For this case, this section is devoted to presenting a new paradigm leading to the prediction of the RPs with two NN-based methods: 1) GAN network to predict the RPs based on the previously defined RPs at various frequencies through extracted RP images, 2) LSTM-based DNN leads to estimate RPs based on the inserted S_{11} specification.

A. GAN network

The general structure of GAN is depicted in Fig. 1 includes the generator network and the discriminator network. In this DNN-based network, random vectors are the input for the generator network leads to having data namely as 'training data'. With the help of this training data and also the produced data from the generator, the discriminator network estimates labels (either real or generated). For training an accurate network and verifying the accuracy in terms of the loss functions, parameters such as filter Size, number of filters, dropout probability, along a number of epochs must be optimized and determined here we use a 'rule of thumb' method for defining these ones. With the help of this network, the RPs of any antenna can be predicted for the determined frequency.

B. LSTM-based DNN

The presented LSTM-based DNN in Fig. 2 is another solution for estimating the RPs in both E and H planes. Here, the S_{11} specification is the input data and the RPs are the output specifications that are estimated by the trained DNN. Like the GAN, the 'rule of thumb' can be used for determining the number of hidden layers with the number of neurons in each one. In this kind of network, the type of hidden layer is LSTM.

III. Practical Implementation of Proposed Methods

The proposed NN-based approaches are validated by designing and optimizing an FSS structure operating at the X-band. This configuration is used for predicting the RPs at a specific frequency (here, 10.5 GHz) [14]. This section is devoted to presenting the practical simulation results achieved from GAN and LSTM-based DNN leads to estimate the RPs.

The general structure of the designed FSS is depicted in Fig. 3. Here firstly a circular patch is designed and afterward, it is divided into sub-sections. The design parameters of the configuration (i.e., geometric parameters) are optimized with the help of a genetic algorithm (GA). The employed optimization method (i.e., GA) will result in optimal variables starting from the smallest circular shapes with a diameter of 2 mm and thickness of 0.5 mm. Then, the next circle shape is enlarged in size with a coefficient of 2. The configuration is executed on FR-4 with relative permittivity ε_r=4.1 and of thickness of 0.5 mm for which L_2=36 mm, W_1=18 mm, and L_1=17.5 mm. The S_{11} performance representation for the designed FSS is presented in Fig. 3 operating as follows: 5.70-5.92 GHz, 7.23-7.52 GHz, 8.24-8.70 GHz, 9.10-9.59 GHz, 10.23-11.05 GHz, and 13.57-13.75 GHz, respectively.

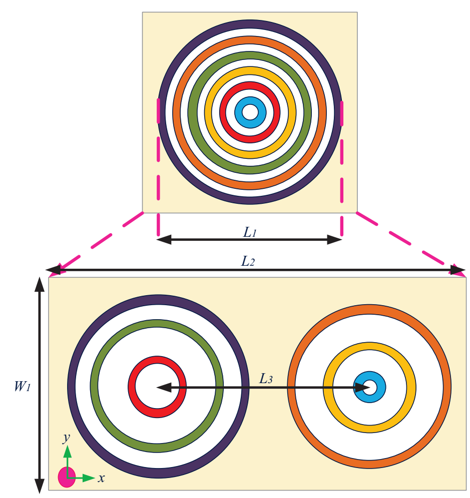

Fig. 3. Structure of FSS employed for training GAN and LSTM-based DNN.

The important step for training any NN is the generation of a suitable amount of training data. For this case, the design parameters of the designed FSS is iterated randomly and for each condition specifications in terms of S-parameter (here, S_{11}) and RPs are achieved. In total 700 RP-based images are extracted for training the GAN and 1000 data are extracted for

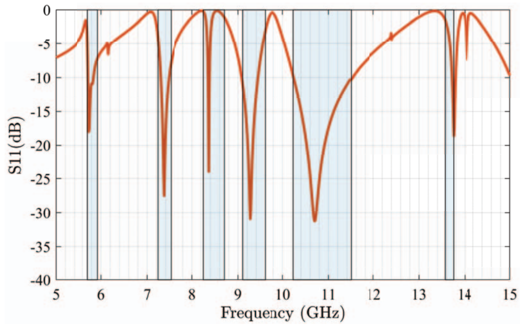

Fig. 4. S_{11} performance of designed FSS configuration.

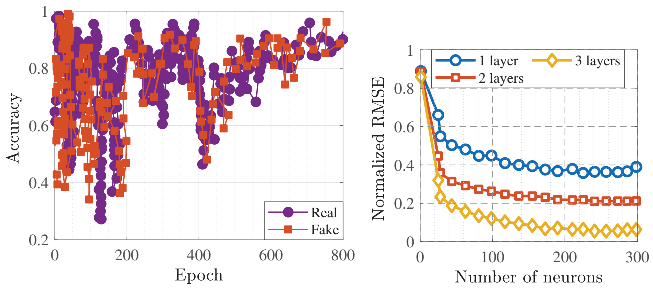

Fig. 5. Accuracy of trained GAN (right) and RMSE representation of trained LSTM-based DNN (left) for the designed FSS structure.

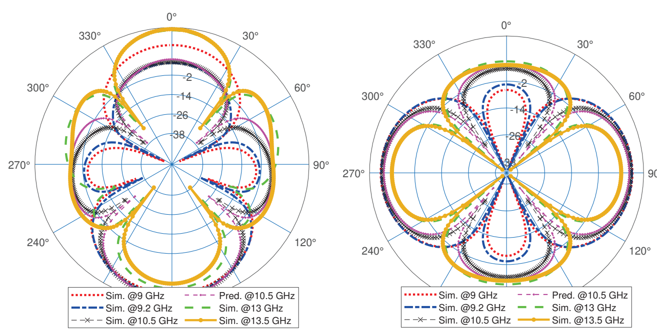

Fig. 6. RPs for designed FSS at $\phi = 0$ (left), and $\phi = 90°$ (right).

constructing the LSTM-based DNN. In the trained GAN, 64 filters are used for both generator and discriminator networks, also the filter size is defined as 5. For the designed FSS, two NNs are trained and the accuracy of trained GAN in terms of the epoch is depicted in Fig. 5-(left). From another point of view, the root mean square error (RMSE) specification is used for presenting the accuracy of the constructed DNN which shows that a 0.087 value is achieved for the trained DNN with 3 hidden layers and 300 neurons in each one, as Fig. 5-(right) shows.

With the trained GAN and LSTM-based DNN, the RPs for both E-plane and H-plane are depicted in Fig. 6. Here, for various frequencies, the RPs are extracted and for 10.5 GHz the RPs are predicted by the GAN and LSTM-based DNN. It is observed that the outcomes achieved from simulation and predictions at 10.5 GHz show a good agreement.

IV. Conclusions

In this work, two methodologies for predicting the RPs are presented — GAN and LSTM-based DNN. For the GAN structure, a suitable amount of RP-based images and for LSTM-based DNN, frequency-based outcomes in terms of S_{11} must be prepared leading to training the networks. The trained networks predict the RPs at the determined frequency(ies) which saves the long-time simulations and helps the designers to extract results much faster. The proposed method is validated by designing and optimizing an FSS structure for which RPs are predicted at the specific frequency and shows great agreement with the simulation results.

References

[1] M. Balasubramanian, S. D. Campbell, D. H. Werner, and T. H. Hand, "A shaped reflector antenna design approach for contoured beam synthesis with surface curvature constraints," *IEEE Transactions on Antennas and Propagation*, vol. 72, no. 2, pp. 1297–1307, 2024.

[2] F. Vaquero, M. R. Pino, and M. Arrebola, "Adaptive field-to-mask procedure for the synthesis of metalens antennas with complex near-field coverage patterns in 5g scenarios," *IEEE Transactions on Antennas and Propagation*, vol. 71, no. 9, pp. 7158–7171, 2023.

[3] S. Zohrevand, M. A. Chaychi Zadeh, E. Farokhipour, D. Erni, and N. Komjani, "A small-aperture and high-performance endfire holographic antenna based on spoof surface plasmon polaritons," *IEEE Antennas and Wireless Propagation Letters*, vol. 23, no. 9, pp. 2743–2747, 2024.

[4] F. Zhao, X. Pan, Q. Xie, X. Meng, and S. Xiao, "A grating lobe suppression method based on convex relaxation iterative optimization in limited-scanning planar array," *IEEE Antennas and Wireless Propagation Letters*, vol. 22, no. 6, pp. 1426–1430, 2023.

[5] R. Kormilainen, A. Lehtovuori, J. Liesiö, and V. Viikari, "A method to co-design antenna element and array patterns," *IEEE Access*, vol. 10, pp. 31 190–31 200, 2022.

[6] Q. Zeng, P. Yang, Y. Man, L. Han, F. Yang, G. Wang, and S. Yang, "A probability-based time-modulated array and its statistical model," *IEEE Antennas and Wireless Propagation Letters*, vol. 22, no. 2, pp. 407–411, 2023.

[7] H. Wang, A. Li, Y.-F. Liu, Q. Qin, L. Song, and Y. Li, "Achievable rate maximization pattern design for reconfigurable mimo antenna array," *IEEE Transactions on Wireless Communications*, vol. 22, no. 9, pp. 5884–5897, 2023.

[8] H. Y. Hou and Y. J. Cheng, "Active-isolation improvement of shared-aperture beam-scanning array based on excitation optimization techniques," *IEEE Antennas and Wireless Propagation Letters*, vol. 23, no. 2, pp. 808–812, 2024.

[9] C. Z. Feng, W. T. Li, C. Cui, Y. Q. Hei, J. C. Mou, and X. W. Shi, "An efficient and universal static and dynamic convex optimization for array synthesis," *IEEE Antennas and Wireless Propagation Letters*, vol. 21, no. 10, pp. 2060–2064, 2022.

[10] X. Zhang, X. Gao, X. Bu, and J. An, "An improved snake optimization algorithm for sparse conformal array beamforming," *IEEE Transactions on Vehicular Technology*, vol. 73, no. 6, pp. 8542–8548, 2024.

[11] X. Li and K. M. Luk, "The grey wolf optimizer and its applications in electromagnetics," *IEEE Transactions on Antennas and Propagation*, vol. 68, no. 3, pp. 2186–2197, 2020.

[12] S. Koziel, N. Çalık, P. Mahouti, and M. A. Belen, "Accurate modeling of antenna structures by means of domain confinement and pyramidal deep neural networks," *IEEE Transactions on Antennas and Propagation*, vol. 70, no. 3, pp. 2174–2188, 2022.

[13] I. Syrytsin, G. F. Pedersen, and S. Zhang, "User effects on mobile phone antennas: Review and potential future solutions," *IEEE Open Journal of Antennas and Propagation*, vol. 5, no. 1, pp. 5–17, 2024.

[14] L. Kouhalvandi and L. Matekovits, "A case study for improving performance of frequency selective surface through union of sub-sets and particle swarm optimization," in *2022 International Conference on Electromagnetics in Advanced Applications (ICEAA)*, 2022, pp. 113–116.